Salivary gland imaging in Sjogren's syndrome

Susan I Lemon,
Steven G Imbesi &
Alexander R Shikhman[†]

[†]*Author for correspondence*
Scripps Clinic, Member of the
Division of Rheumatology,
MS113, 10666 North Torrey,
Pines Road, La Jolla,
CA 92037, USA
Tel.: +1 858 554 8562;
Fax: +1 858 554 6763;
ashikhman@scrippsclinic.com

Sjogren's syndrome (SS) is a systemic connective tissue disease characterized by a progressive immune-mediated impairment of the exocrine glands. The high prevalence in the general population of sicca and other symptoms mimicking SS has increased the need for accurate tools in its diagnosis. Imaging may be substantially helpful in this regard, as well as in the assessment of acute and chronic complications of the disease. A future application of salivary imaging in SS may be guiding therapeutics by enabling radiographic monitoring of treatment responsiveness. This review of salivary gland imaging in SS summarizes the types of information yielded by currently available modalities and suggests their proper clinical application. It emphasizes recent advances in noninvasive imaging, including magnetic resonance sialography, ultrasonography and nuclear medicine techniques.

Sjogren's syndrome (SS) is a systemic connective tissue disease characterized by a progressive immune-mediated impairment of the exocrine glands [1,2]. Common clinical manifestations of exocrine involvement in SS include keratoconjunctivitis sicca, xerostomia and episodic glandular swelling. SS affects 1–4 million people in the USA, has a significant female predominance and has a peak incidence between the ages of 40 and 60 years [3].

Salivary glands are one of the key target organs affected by SS [4]. Morphologically, normal salivary glands consist of secretory units, which include acini (cells producing primary secretion), myoepithelial cells (cells moving secretions toward the excretory duct), the intercalated ducts (the ducts lined with low cuboidal epithelial cells rich in carbonic anhydrase and secreting bicarbonate into the ductal lumen while absorbing chloride from the lumen), the striated ducts (the ducts lined with simple cuboidal epithelial cells absorbing Na$^+$ from the lumen and secreting K$^+$ into the lumen), and the excretory ducts (ducts lined with simple cuboidal epithelium proximally and stratified cuboidal or pseudostratified columnar epithelium distally and not performing any modification of the saliva). While lymph nodes are commonly present within the parotid glands, lymphoid infiltrates are absent in all normal salivary tissue [5–7].

The pathomorphological hallmark of SS is lymphocytic infiltration of the salivary glands with predominantly CD4$^+$ T cells [1]. In the early stages of SS, lymphocytic infiltration results in thinning and fragmentation of the connective tissue reticulum of the terminal or intercalated duct walls. As the disease progresses, this accumulation continues, the serous acini become surrounded, compressed,

future medicine part of fsg

atrophic and, finally, destroyed [8]. Eventually, the only remaining ductal epithelium consists of isolated cell clusters of epithelial and myoepithelial cells surrounded by a dense lymphocytic infiltration (a benign lymphoepithelial lesion) [9]. These pathological changes lead to salivary gland hypofunction, including decreased salivary gland flow, increased saliva viscosity, as well as abnormal salivary biochemistry, bactericidal and fungicidal properties [10]. Salivary gland involvement in SS may manifest clinically as recurrent gland swelling, xerostomia, increased frequency of dental caries and oral candidiasis, gingival recession, fissuring of the tongue, angular cheilitis, halitosis, dysphagia and hoarseness of voice [3].

Although minor salivary gland biopsy yielding a focus score of 1 or greater is still considered a diagnostic gold standard for SS, salivary gland imaging has significant value in the evaluation of SS owing to the disease predilection for glandular involvement [11]. Imaging may help to correctly classify patients with sicca symptoms by differentiating between SS versus non-SS causes of dryness. It can be used to differentiate palpable or painful salivary gland abnormalities of SS from other conditions in the differential diagnosis (**Box 1**). Specifically, different imaging modalities lend valuable information about salivary anatomy and/or function. Conventional modalities have included sialography and scintigraphy. In recent years, there has been considerable development in the use of ultrasonography and magnetic resonance imaging (MRI) for the evaluation of salivary glands. The current review summarizes published data on imaging modalities used in differential diagnosis and functional assessment of salivary glands in SS.

Box 1. Differential diagnosis of salivary involvement in Sjogren's syndrome.

- Benign sialectasis
- Sialolithiasis
- Chronic sialadenitis
- Infection
  – Bacterial (i.e., *Staphylococcus aureus*), viral (i.e., HIV, hepatitis C virus and mumps)
- Tumors
- Granulomatous diseases
  – Tuberculosis, nontuberculous *Mycobacterium*, sarcoidosis, syphilis, cat-scratch fever and fungal infections
- Vasculitis (Wegener's granulomatosis)
- Sialosis
  – Diabetes mellitus, alcoholism, hypothyroidism, malnutrition, diuretics and psychotropics
- Chronic graft-versus-host disease
- Amyloidosis
- Eating disorders

Modalities

Plain sialography and MRI provide anatomical detail via static images but do not assess function (**Table 1**). MRI offers advantages over sialography including its noninvasive nature and ability to provide high-resolution images of salivary gland parenchyma. Sialography shows salivary duct architecture, but is an invasive procedure which can be painful and, particularly in the setting of acute sialadenitis, predispose to infection and induce obstruction. Nuclear medicine technetium-99m pertechnetate (^{99m}Tc)-based scintigraphy yields dynamic information by quantifying salivary flow rates but does not provide anatomical information. Ultrasound (US) is a modality which boasts relatively inexpensive, noninvasive acquisition of structure and function. High-resolution US images are now readily available with the use of modern very-high frequency transducers. Combination techniques, such as magnetic resonance (MR) sialography and sialographic sonography, have been developed with hopes of increasing diagnostic accuracy in SS (**Table 2**). These modalities allow simultaneous imaging of the parenchyma and ducts [12]. While sialographic sonography has not yet been developed for clinical use, MR sialography is being increasingly utilized clinically. Scintigraphy and high-resolution power Doppler US provide objective functional assessments of salivary glands, which can be used as outcome measures in SS clinical trials. The breadth of nuclear medicine evaluation of salivary gland involvement in SS extends beyond conventional scintigraphy to positron emission tomography (PET), PET-computed tomography (CT) and ^{67}Gallium scanning. These tests provide a unique functional assessment by displaying flow and distribution of radioactive tracer but the considerable expense and need for a local isotope-producing cyclotron limits their practicality.

Sialography

Sialography is an invasive test performed by cannulating the main ducts of major salivary glands via their oral mucosal orifices and infusing contrast retrograde to the usual direction of salivary flow. Stensen's duct of the parotid gland enters the mouth along the buccal mucosa adjacent to the upper second molar, and Wharton's duct of the submandibular gland drains into the floor of the mouth near the frenulum. The main intercalated ducts branch into peripheral ducts which end in acini. Sialography outlines salivary duct anatomy and provides reliable results in the diagnosis of SS that challenge the current gold standard of minor salivary gland biopsy. Secretory sialography adds the ability to perform functional assessment of salivary glands (**Table 1**). Sialography is included in both the Japanese and European Community criteria for the diagnosis of SS [13].

Sialography of parotid and submandibular glands readily differentiates the pseudosialectasis of SS from chronic sialadenitis, sialolithiasis, granulomatous conditions, tumors and the sialoses (**Box 1**). Historically, SS signature sialographic staining pattern was that of patent, nondilated main ducts with diffusely uniform punctuate or globular collections throughout the gland [14]. These collections were thought to be

Table 1. Characteristics of imaging modalities in Sjogren's syndrome.

Modality	Anatomy	Function
Sialography	(+)	(-)
Secretory sialography	(+)	(+)
Scintigraphy, PET	(-)	(+)
PET-CT	(+)	(+)
MRI, MR sialography	(+)	(-)
Dynamic MR Sialography	(+)	(+)
US	(+)	(-)
Power Doppler US	(+)	(+)

+: Informative; -: Noninformative.
CT: Computed tomography; MRI: Magnetic resonance imaging; PET: Positron emission tomography; US: Ultrasound.
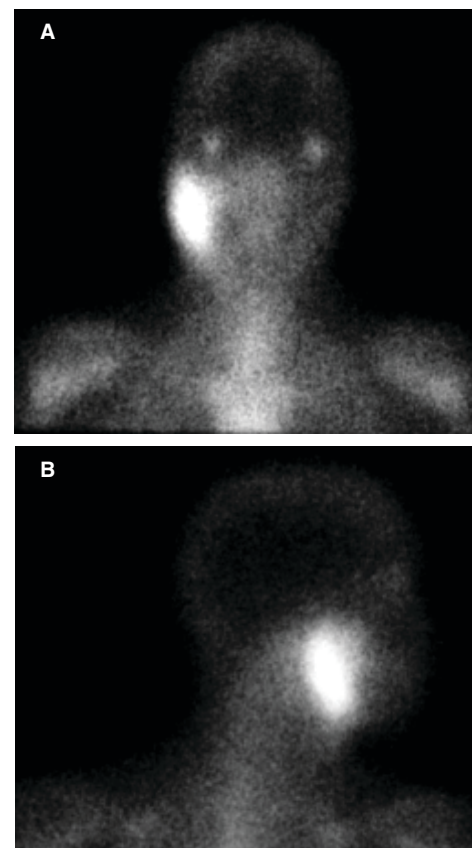
Table 2. Sensitivity and specificity of imaging modalities for Sjogren's syndrome.

Modality	Sensitivity (%)	Specificity (%)	Ref.
Sialography	87	98	[16]
Scintigraphy	87.2	79	[53]
	85	78	[19]
Magnetic resonance imaging	93.9	97.8	[30]
	81	100	[36]
Magnetic resonance sialography	96	100	[36]
	96	100	[48]
Ultrasound	76	94	[16]
	58.8	98.7	[32]
	89.8	93.6	[30]
	78	94	[36]

Different classification criteria and technologies may be reflected among studies.

artifacts of the sialographic procedure that represented contrast material extravasating outside the duct lumen through weakened duct walls [14].

Figure 1. ^{67}Gallium accumulation in the right parotid and bilateral lacrimal glands in a patient with primary Sjogren's syndrome.

(A) Anterior–posterior view **(B)** Right lateral view.

However, with the advent of MR sialography, a noncontrast modality, these punctate or globular collections were found to be actual dilated peripheral ducts rather than artifact. Cavitary and destructive pseudosialectasis accompany further disease progression and reflect complications of infection. They range from irregular, larger globules that are nonuniformly distributed with deformed, dilated main ducts to unrecognizable peripheral duct branching [14]. These findings are in contrast to those of gland enlargement with normal ducts of sialoses, and in agreed with duct dilation and architectural alteration of chronic sialadenitis [15].

Yonetsu and colleagues found on multivariable analysis that sialography, but not functional or serologic criteria, showed a significant correlation with a positive diagnosis of SS [16]. Yousem and colleagues have suggested its use in staging SS, since patients' symptoms may not correlate well with disease severity [17]. Despite its invasive nature, sialography was well tolerated and had low morbidity in a Netherlands study by Kalk and colleagues, who noted no signs of overfilling or false routes in any of the sialograms, which generally took 12 min to perform and infused 0.74 ml of contrast fluid at a rate of 0.01 ml/s [18]. The technique requires manual skill related to cannulation and an experienced interpreter. It should be avoided in acute sialadenitis owing to concern for the potentiation of infection, obstruction due to instrumentation or initiating duct rupture [17].

Scintigraphy
Scintigraphy is a nuclear medicine test which measures salivary gland uptake and secretion of radionucleotide isotope ^{99m}Tc following its intravenous injection. Included in the 1976 Copenhagen criteria and the European Community criteria, scintigraphy is a noninvasive modality with which to quantitate salivary flow rates and thereby obtain a functional assessment. It has been shown to differentiate between SS and healthy controls, and, further, between Sjogren's and non-Sjogren's sicca symptoms [19]. Scintigraphic findings that characterize SS are low uptake of the radionucleotide and, in severe cases, inability to detect tracer in the salivary ductal system. Umehara and colleagues evaluated salivary gland disease in SS using quantitative salivary scintigraphy with lemon juice stimulation [20]. They found that decreased secretion velocity in the parotid gland and decreased accumulation in the submandibular gland were sensitive indicators of salivary gland disease in
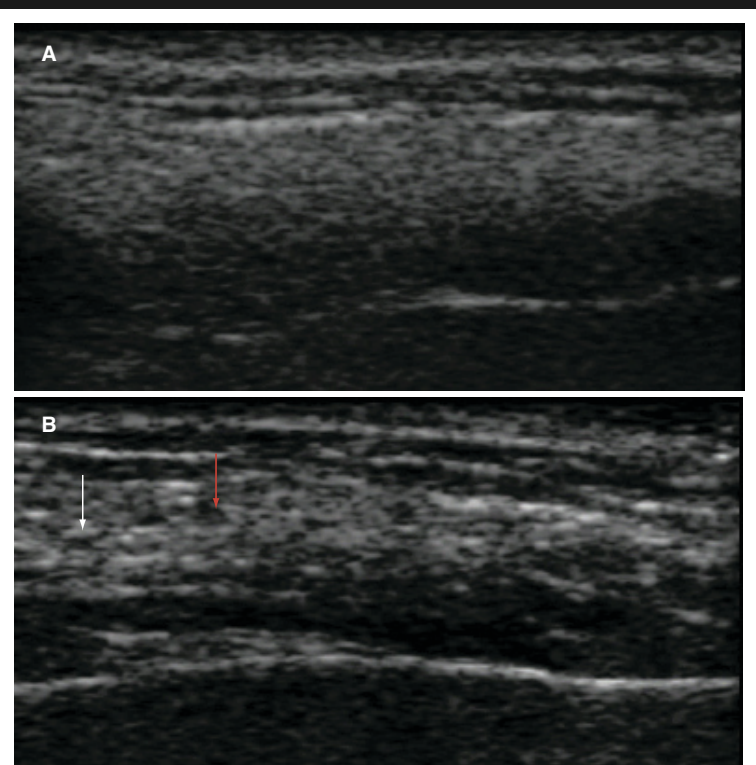
Table 3. Sensitivity, specificity and accuracy of distinct sonographic features in salivary gland screening for Sjogren's syndrome.

Sonographic findings	Sensitivity (%)	Specificity (%)
Parotid glands		
P1 Multiple hypoechoic areas	88.4	80.6
P2 Multiple hyperechoic lines and/or spots	93.0	94.4
P3 Multiple hypoechoic areas surrounded with hyperechoic lines and/or spots	46.5	100
Submandibular glands		
S1 Multiple hypoechoic areas	86.0	75.0
S2 Multiple hyperechoic lines and/or spots	62.8	91.7
S3 Multiple hypoechoic areas surrounded with hyperechoic lines and/or spots	41.9	97.2
S4 Obscured gland configuration	46.5	97.2

Shimizu et al. [38]

SS; these parameters were correlated with histopathological grading of labial biopsy and with sialographic findings [20,21]. In patients with primary and secondary SS, submandibular gland

Figure 2. Ultrasonography of salivary glands in Sjogren's syndrome.

The sonographic images, obtained using a 10 MHz linear transducer, illustrate hypoechoic areas (red arrow) and hyperechoic bands (white arrow) in the parotid gland of a patient with Sjogren's syndrome (SS). **(A)** Normal parotid gland. **(B)** Parotid gland affected by SS.

scintigraphies have shown more pathological results than parotid [21]. Additionally, scintigraphy results have shown more severe functional deficits in those patients with secondary compared with primary SS [21].

In 2003, Shizukuishi and colleagues developed a scintigraphic scoring system based on excretion rates of salivary glands after dynamic scintigraphy with vitamin C stimulation in patients with SS which ranged from 0–3; 0 represents normal function and excretion rates of greater than 50% while 3 represents severe dysfunction and excretion rates of less than 25% [22]. They then validated the scoring system against the Saxon test, a functional test which involves weighing a sponge before and after it is chewed for 2 min, which has a sensitivity and specificity of 70 and 71%, respectively [16,23]. As with sialography, experience is crucial to an accurate interpretation of scintigraphy.

[67]Gallium is another radiotracer available for use in the diagnosis of SS [24]. [67]Gallium acts as an iron analog. Initially, it binds to transferrin and diffuses through loose endothelial junctions of capillaries at sites of inflammation, where it enters the extracellular compartment. Leukocytes migrate to sites of inflammation and degranulate, releasing large quantities of lactoferrin. [67]Gallium has a higher affinity for lactoferrin than transferrin, which results in selective accumulation of the isotope in the inflammatory foci [25]. Various patterns of enhanced [67]Gallium accumulation in salivary glands have been demonstrated in SS [24]. Symmetric retention of [67]Gallium in salivary and lacrimal glands, known as the panda sign, has been described in patients with SS and sarcoidosis [26,27]. **Figure 1** demonstrates markedly increased [67]Gallium activity in the right parotid and bilateral lacrimal glands of a 42-year-old woman with primary SS.

Positron emission tomography

PET with ^{18}F-fluorodeoxyglucose utilizes a principle of excessive accumulation of radioactive tracer in areas of inflammation secondary to enhanced glucose transport in activated immune cells. PET combines CT and nuclear scanning; it produces images less detailed than conventional CT or MRI, but is excellent in localizing areas of inflammation. PET-CT complements PET by adding enhanced anatomic detail to this traditionally functional nuclear medicine modality (**Table 1**). PET-CT has recently been employed in demonstrating the inflammatory involvement of salivary glands in

a patient with primary SS [28]. Findings were that of symmetric, intensely hypermetabolic submandibular and parotid salivary glands.

Ultrasonography

As the superficial location of salivary glands lends nicely to sonography, US has become increasingly utilized in the diagnosis, ongoing evaluation, treatment monitoring and lymphoma surveillance of SS. Studies have and continue to be performed using high-resolution, gray-scale power Doppler and color Doppler ultrasonography (CDS) to analyze salivary flow, gland morphology and vascularity. Sonography has been found to perform as well as sialography in differentiating between parotid glands affected by SS and normal glands (**Table 2**) [16]. It accurately differentiates extraglandular from intraglandular lesions [29]. Scoring systems for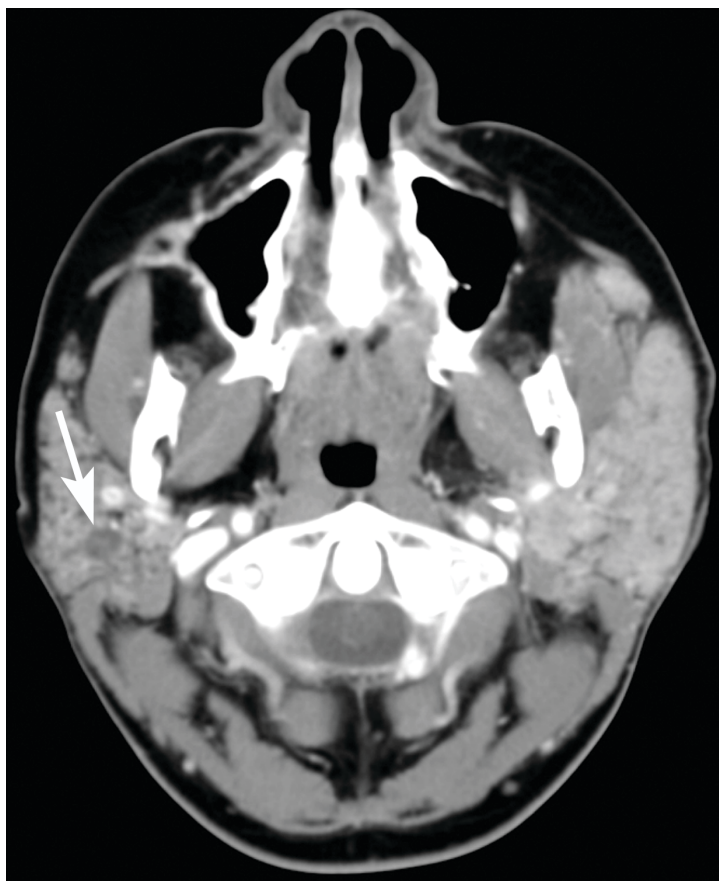 salivary gland US in SS have been developed, correlated with histopathological scores of minor salivary glands and sialographic grading, and their use in SS diagnostics touted [30–33]. Parameters of such scoring systems include parenchymal homogenicity, echogenicity, gland size and posterior gland border. US is limited in its ability to evaluate deep parotid masses and to delineate the course of the facial nerve with respect to tumors [17].

Parotid gland echo structure is normally homogeneous and comparable with the thyroid gland in echogenicity [34]. The submandibular gland is lower than the thyroid in echogenicity. Normal major salivary glands have increased echogenicity relative to adjacent muscle [35]. The parotid's main duct, Stensen's duct, is only rarely visualized in a nondilated state, similar to the main submandibular duct, Wharton's duct. Heterogeneous or nodular parenchyma is regarded as the most accurate sonographic finding of SS patients' salivary glands [36]. Early stage SS is characterized by glandular enlargement followed by hypo- and hyper-echoic foci and inhomogeneity (**Figure 2**) [34]. Cystic spaces reflect progressive glandular destruction and prominent intraglandular sialectasis [37]. Chronic SS typically reveals fibrotic, atrophic glands with accentuated inhomogeneity and multiple hyperechoic bands [34]. It has been demonstrated that pathological sonographic features of salivary glands can be utilized as sensitive and specific tools for SS screening (**Table 3**) [38].
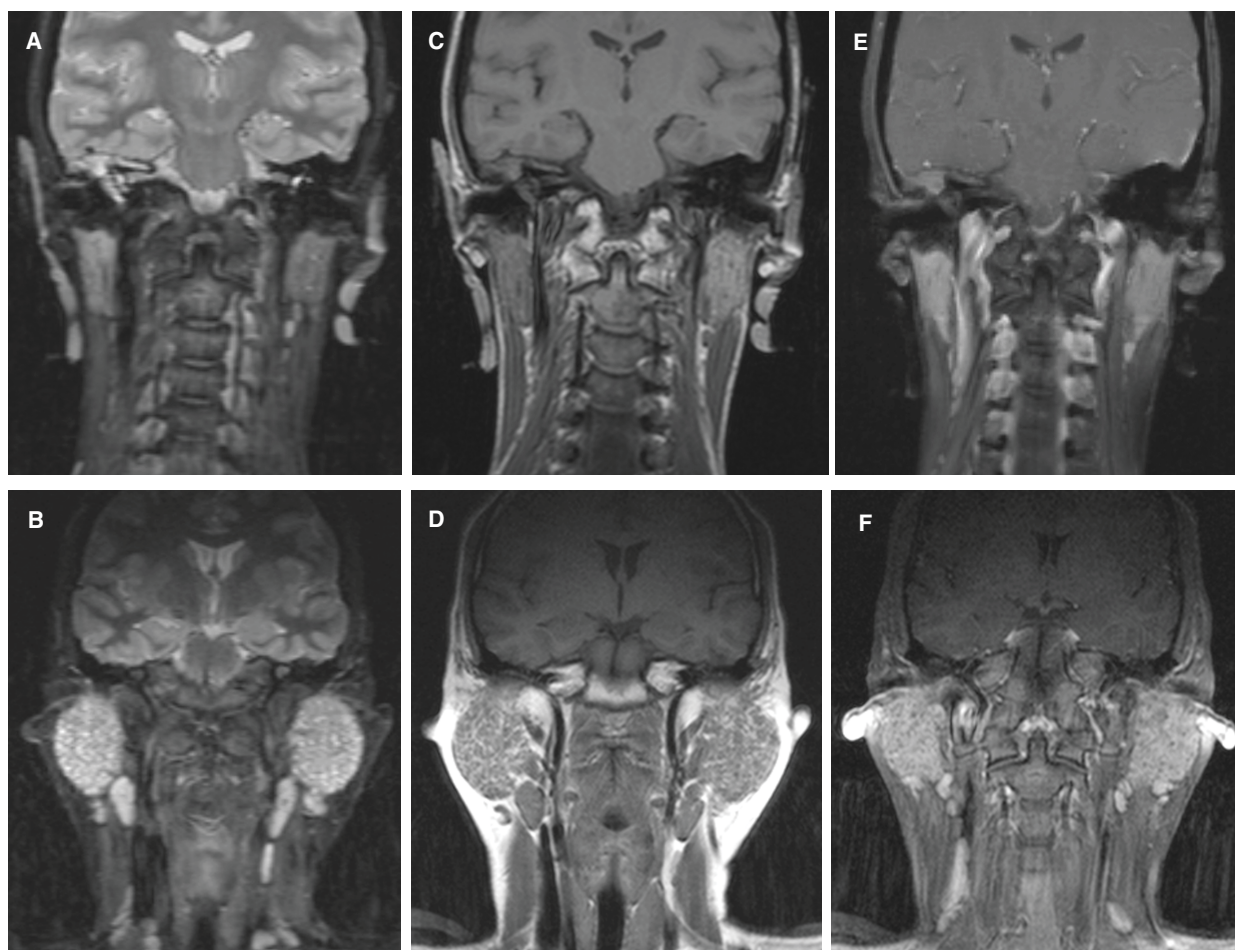
Sonographic findings of SS may resemble those of other conditions but can typically be differentiated with clinical correlation and, if necessary, biopsy (**Box 1**). Sarcoidosis may present as a painless parotid or submandibular lump with sonographic features of coarse, hypoechoic glands [39]. Core biopsy can confirm infiltration with sarcoid granulomata, thereby differentiating sarcoidosis from SS and obviating the need for surgical excision.

Objective quantification of residual salivary gland function and therapeutic response to treatment may comprise US's niche in SS. CDS is useful in evaluating salivary gland vascular anatomy, changes in blood flow occurring during salivary stimulation in normal subjects and flow alterations in the diseased glands of SS [40]. It is acknowledged that intense hyperemia, up to five-times over baseline, normally accompanies salivary secretion [41]. CDS has shown salivary gland hypervascularization in early inflammatory stages of SS. In chronic fibrotic stages, characterized by impaired salivary function, CDS has shown diminished arterial blood flow

Figure 3. Computerized tomography of salivary glands in Sjogren's syndrome.

Axial computed tomography scan demonstrates both microcystic and macrocystic (arrow) changes within the bilateral parotid glands compatible with a subacute to chronic disease state of Sjogren's syndrome.

Figure 4. Magnetic resonance imaging of salivary glands in Sjogren's syndrome.

(A) Normal T2-weighted coronal magnetic resonance imaging (MRI). **(B)** T2-weighted coronal MRI of a patient with Sjogren's syndrome (SS) depicts marked bilateral parotid enlargement as well as multiple high signal foci within the glands due to diffuse microcystic changes. Additional lesions were also identified in the submandibular glands (not included in this image). **(C)** Normal T1-weighted coronal MRI.
(D) T1-weighted coronal MRI again demonstrates the bilateral parotid enlargement and microcystic change compatible with SS.
(E) Normal T1-weighted post-contrast MRI. **(F)** T1-weighted post-contrast MRI shows enhancement throughout the parotid glands, but lack of enhancement in the small cystic lesions, characteristic of SS.

reaction to stimulation [42]. Peak systolic velocity (PSV) is the most sensitive CDS parameter used in detecting vascular changes in major salivary glands in SS. In a study examining blood flow alterations occurring in salivary glands of patients with primary SS, Carotti and colleagues measured the PSV for each waveform at the external carotid artery in the examination of the parotids, and at the facial artery within the submandibular glands before and during lemon juice stimulation [43]. Findings were correlated with the degree of chronic inflammatory changes on minor salivary gland biopsy. In contrast to the statistically significant increase in PSV noted during the stimulation test in controls and SS patients with mild chronic sialadenitis (CS), no significant changes in the PSV values were found with salivary stimulation in the SS patients with severe CS. This illustrates the impaired ability of patients with severe SS to induce an increase in blood flow during stimulation.

Owing to the increased incidence of lymphoma among SS patients, tumor surveillance is a necessary part of their rheumatological care. US and MR imaging can help in identifying dominant masses, which then require aspiration or biopsy [17]. Current recommendations are for biopsy of hypoechogenic lesions of greater than 2 cm and of all fast-growing lesions [34]. The echotexture of lymphoma is finer than in benign adenopathy [44].

Computed tomgraphy

Nonenhanced CT, similar to conventional radiography and US, enables the identification of calculi predisposed by SS [17]. Salivary gland CT in SS initially shows increased gland density and, therefore, increased CT attenuation corresponding to lymphocyte invasion into the gland. It then shows decreased density and decreased CT attenuation representative of tissue destruction, fibrosis and subsequent increased areas of fat deposition which parallels disease severity [45]. In early SS, CT shows diffuse, millimeter-sized fluid density cystic lesions, while in late SS macrocystic changes and solid enhancing nodules due to lymphoid aggregates are identified (Figure 3). CT sialography allows visualization of gland parenchyma as well as ductal structures [46]. In a study of 36 patients, Stone and colleagues found that CT sialography provided little additional useful information over conventional sialography in cases of suspected parotid inflammatory disease. Rather, its value lies in distinguishing intrinsic from extrinsic lesions, differentiating benign from malignant tumors and determining the relationship of these tumors to the facial nerve [46]. CT sialography has largely been replaced by MR sialography.

MRI & MR sialography

MRI yields high-resolution images of salivary and lacrimal gland parenchyma. Its results have been validated against histopathological scores as well as sialography scores [30]. Kawai and colleagues found that the apparent diffusion coefficients of lacrimal glands in SS were significantly lower than those from normal glands of age-matched healthy volunteers, suggesting its utility in assessing lacrimal glands in SS [47]. Using fat suppression MRI (short inversion time inversion recovery and fat-saturation), Izumi and colleagues demonstrated an association between SS and premature salivary gland fat deposition and showed that these changes correspond to the severity of salivary flow dysfunction [45]. Criteria for staging severity of parotid gland disease have been derived using quantitative MR imaging of fat, intact gland lobules, and a number of sialoectatic foci [48]. Figure 4 demonstrates bilateral parotid enlargement and microcystic changes seen by MR imaging in a patient with SS compared with a healthy subject.

Heavily T2-weighted MRI sequences with fat suppression are effectively a method of noninvasive sialography and can delineate ductal pathology, as seen using traditional sialography (Figure 5). Similar information to conventional sialography can be gleaned with MR sialography without requiring cannulation, contrast medium or ionizing radiation, leading to its increased popularity [49]. Patterns obtained at MR sialography correlated well with results of minor salivary gland biopsy [49]. When used in combination, T1-weighted and fat-suppressed T2-weighted images and MR sialography yielded high sensitivity and specificity of 96 and 100%, respectively (Table 2). Accordingly, MR imaging clearly differentiated between SS and non-SS etiologies of xerostomia. MR sialography has heightened sensitivity over CT to salivary gland edema [17]. MRI and MR sialography have better sensitivity and specificity for SS than any other imaging modality but carry drawbacks of significant cost and usual MR contraindications (Table 2).

Recently introduced dynamic MR sialography permits monitoring of salivary gland function [50]. This technique relies upon the acquisition of the optimal section using 2D fast asymmetric spin-echo sequencing, with single-section acquisition of thick sections repeated every 30 s before and after stimulation of salivation with 5% citric acid. The actual assessment of salivary gland function is based on time-dependent changes in the area of the detectable parotid gland's main ducts and

Figure 5. Magnetic resonance sialogram of the parotid gland in Sjogren's syndrome.

Sagittal maximum intensity projection reconstruction magentic resonance sialogram of the parotid gland demonstrates multiple millimeter and submillimeter high signal intensity intraglandular collections of fluid consistent with Sjogren's syndrome. There is also diffuse dilatation of Stensen's duct with associated foci of stenosis (arrows).

high-intensity linear structures from the parotid glands to the upper first molar region before and after citric acid stimulation [50]. Dynamic MR sialography was shown to discriminate between the salivary gland function of SS patients and healthy subjects [51].

MR imaging is also utilized in identifying dominant masses within glands affected by SS. It is particularly valuable in suggesting the need for aspirations or biopsies of these dominant masses in SS given the 4400% increased risk of parotid lymphoma in this population [52].

Conclusion & future perspective

An expanding selection of diverse imaging modalities capable of assessing salivary gland anatomy and function has created a solid basis for their use in the diagnosis and surveillance of SS.

We expect that the future role of imaging techniques in SS will include:

- Their broader utilization in the initial and differential diagnoses;
- Prospective surveillance of the salivary gland residual function;
- Lymphoma screening and surveillance;
- Prediction and monitoring of therapeutic responses to salivary secretagogues;
- Monitoring of therapeutic responses to disease modifying antirheumatic drugs and biologics;
- Development and introduction into routine practice of high-resolution 3D US tomography, which will combine gray-scale and Doppler images of the glandular parenchyma, vasculature and ductal anatomy with blood and saliva flow parameters.

Executive summary

- Imaging is an integral part of Sjogren's syndrome (SS) diagnostics, staging, functional assessment and tumor surveillance.

- High-resolution ultrasound is the imaging modality of choice in many clinical situations, allowing noninvasive assessment of both structure and function in SS when Doppler is performed.

- Nuclear medicine-based scintigraphy and positron emission tomography scans provide sensitive functional assessments of salivary glands in SS.

- Computed tomography is particularly useful in evaluating for the presence of sialolithiasis and the evaluation of masses.

- Sialography assesses salivary gland duct abnormalities; noninvasive magnetic resonance sialography adds simultaneous visualization of gland parenchyma and may soon replace conventional x-ray sialography.

- Future uses of imaging, aside from diagnosis, may include directing therapeutics and monitoring therapeutic responses.

Bibliography

Papers of special note have been highlighted as either of interest (•) or of considerable interest (••) to readers.

1. Larche MJ: A short review of the pathogenesis of Sjogren's syndrome. *Autoimmun. Rev.* 5(2), 132–135 (2006).

2. Theander E, Manthorpe R, Jacobsson LT: Mortality and causes of death in primary Sjogren's syndrome: a prospective cohort study. *Arthritis Rheum.* 50(4), 1262–1269 (2004).

3. Hsu S, Dickinson D: A new approach to managing oral manifestations of Sjogren's syndrome and skin manifestations of lupus. *J. Biochem. Mol. Biol.* 39(3), 229–239 (2006).

4. Chisholm DM, Mason DK: Salivary gland function in Sjogren's syndrome: a review. *Br. Dent. J.* 135(9), 393–399 (1973).

5. Pinkstaff CA: The cytology of salivary glands. *Int. Rev. Cytol.* 63, 141–261 (1979).

6. Garrett JR: Recent advances in physiology of salivary glands. *Br. Med. Bull.* 31(2), 152–155 (1975).

7. Mandel ID, Wotman S: The salivary secretions in health and disease. *Oral Sci. Rev.* 8, 25–47 (1976).

8. de Wilde PC, Vooys GP, Baak JP *et al.*: Quantitative immunohistologic and histomorphometric diagnostic criteria for Sjogren's syndrome. *Pathol. Res. Pract.* 185(5), 778–780 (1989).

9. Ihrler S, Zietz C, Sendelhofert A, Riederer A, Lohrs U: Lymphoepithelial duct lesions in Sjogren-type sialadenitis. *Virchows Arch.* 434(4), 315–323 (1999).

10. Sreebny LM: Saliva in health and disease: an appraisal and update. *Pathol. Res. Pract.* 50(3), 140–161 (2000).

11. Bodeutsch C, de Wilde PC, Kater L *et al.*: Quantitative immunohistologic criteria are superior to the lymphocytic focus score criterion for the diagnosis of Sjogren's

syndrome. *Arthritis Rheum.* 35(9), 1075–1087 (1992).

12. Shimizu M, Tokumori K, Okamura K *et al.*: Possibility of sialographic sonography: a Doppler phantom study. *Oral Surg. Oral Med. Oral Pathol. Oral Radiol. Endod.* 91(6), 719–727 (2001).

13. Manthorpe R, Jacobsson L: Sjogren's syndrome. In: *Bailliere's Clinical Rheumatology: Classification and Assessment of Rheumatic Diseases: part II.* Silman AJ, Symmons DPM (Eds). Bailliere Tindall, London, UK, 9(3) 483–496 (1995).

•• Very useful review for those involved in the design of Sjogren's syndrome (SS) clinical trials.

14. Som PM, Shugar JM, Train JH, Biller HR: Manifestations of parotid gland enlargement: radiographic, pathologic, and clinical correlations. I. The autoimmune pseudosialectasias. *Radiology* 141, 415–419 (1981).

15. Som PM, Shugar JM, Train JS, Biller HF: Manifestations of parotid gland enlargement: radiographic, pathologic, and clinical correlations. II. The disease of Mikulicz syndrome. *Radiology* 141, 421–426 (1981).

16. Yonetsu K, Takagi Y, Sumi M, Nakamura T, Eguchi K: Sonography as a replacement for sialography for the diagnosis of salivary glands affected by Sjögren's syndrome. *Ann. Rheum. Dis.* 61, 276–286 (2002).

17. Yousem DM, Kraut MA, Chalian AA: Major salivary gland imaging. *Radiology* 216(1), 19–29 (2000).
•• Basics of salivary gland imaging.

18. Kalk WW, Vissink A, Spijkervet FK, Moller JM, Roodenburg JL: Morbidity from parotid siaglography. *Oral Surg. Oral Med. Oral Pathol. Oral Radiol. Endod.* 92(5), 572–575 (2001).

19. Tensing EK, Nordstrom DC, Solovieva S *et al.*: Salivary gland scintigraphy in SS and patients with sicca symptoms but without SS: the psychological profiles and predictors for salivary gland dysfunction. *Ann. Rheum. Dis.* 62, 964–968 (2003).

20. Umehara I, Yamada I, Murata Y, Takahashi Y, Okada N, Shibuya H: Quantitative evaluation of salivary gland scintigraphy in Sjögren's Syndrome. *J. Nucl. Med.* 40(1), 64–69 (1999).

21. Aung W, Yamada I, Umehara I, Ohbayashi N, Yoshino N, Shibuya H: Sjögren's syndrome: comparison of assessments with quantitative salivary gland scintigraphy and contrast sialography. *J. Nucl. Med.* 41(2), 257–262 (2000).

22. Shizukuishi K, Nagaoka S, Kinno Y *et al.*: Scoring analysis of salivary gland scintigraphy in patients with Sjögren's syndrome. *Ann. Nucl. Med.* 17(8), 627–631 (2003).
• Detailed approach to scintigraphy of salivary glands in SS.

23. Kohler PF, Winter ME: A quantitative test for xerostomia. The Saxon test, an oral equivalent of the Schirmer test. *Arthritis Rheum.* 28, 1128–1132 (1985).

24. Collins RD Jr, Ball GV, Logic JR: Gallium-67 scanning in Sjögren's syndrome: concise communication. *J. Nucl. Med.* 25(3), 299–302 (1984).

25. Hoffer P: Gallium: mechanisms. *J. Nucl. Med.* 21, 282–285 (1980).

26. Sulavik SB, Spencer RP, Castriotta RJ: Panda sign – avid and symmetrical radiogallium accumulation in the lacrimal and parotid glands. *Semin. Nucl. Med.* 21(4), 339–340 (1991).

27. Kurdziel KA: The panda sign. *Radiology* 215(3), 884–885 (2000).

28. Jadvar H, Bonyadlou S, Iagaru A, Colletti PM: FDG PET-CT demonstration of Sjögren's sialoadenitis. *Clin. Nucl. Med.* 30(10), 698–699 (2005).

29. Gritzmann N: Sonography of the salivary glands. *Am. J. Roentgenol.* 153, 161–166 (1989).

30. Miedany YM, Ahmed I, Mourad HG *et al.*: Quantitative ultrasonography and magnetic resonance imaging of the parotid gland: can they replace the histopathologic studies in patients with Sjögren's syndrome? *Joint Bone Spine* 71, 29–38 (2004).

31. Salaffi F, Argalia G, Carotti M, Giannini FB, Palombi C: Salivary gland ultrasonography in the evaluation of primary Sjögren's syndrome. Comparison with minor salivary gland biopsy. *J. Rheum.* 23, 1229–1236 (2000).

32. Hocevar A, Ambrozic A, Rozman B, Kveder T, Monsic M: Ultrasonographic changes of major salivary glands in primary Sjögren's syndrome. Diagnostic value of a novel scoring system. *Rheumatology* 44, 768–722 (2005).
•• Systematic approach to salivary gland sonography in SS.

33. Makula E, Pokorny G, Raijtar M, Kiss I, Kovacs A, Kovacs L: Parotid gland ultrasonography as a diagnostic tool in primary Sjögren's syndrome. *Br. J. Rheumatol.* 35, 972–977 (1996).

34. Gritzmann N, Rettenbacher T, Hollerweger A, Macheiner P, Hubner E: Sonography of the salivary glands. *Eur. Radiol.* 13, 964–975 (2003).

35. Seibert RW, Seibert JJ: High-resolution ultrasonography of the parotid gland in children. *Periatr. Radiol.* 16, 374–379 (1986).

36. Niemela RK, Takalo R, Paakko E *et al.*: Ultrasonography of salivary glands in primary Sjögren's syndrome. A comparison with magnetic resonance imaging and magnetic resonance sialography of parotid glands. *Rheumatology* 43(7), 875–879 (2004).

37. Martinoli C, Derchi LE, Solbiati K, Rizzatto G, Silvestri E, Giannoni M: Colour Doppler sonography of salivary glands. *Am. J. Roentgenol.* 163, 933–941 (1994).

38. Shimizu M, Okamura K, Yoshiura K, Ohyama Y, Nakamura S, Kinukawa N: Sonographic diagnostic criteria for screening Sjögren's syndrome. *Oral Surg. Oral Med. Oral Pathol. Oral Radiol. Endod.* 102(1), 85–93 (2006).

39. Howlett DC, Alyas F, Wong KT *et al.*: Sonographic assessment of the submandibular space – Pictoral Review. *Clin. Radiol.* 59, 1070–1078 (2004).
• Good reference of salivary ultrasound images.

40. Martinoli C, Derchi LE, Solbiati L, Rizzatto G, Silvestri E, Giannoni M: Color Doppler sonography of salivary glands. *Am. J. Roentgenol.* 163, 933–941 (1994).

41. *Fisiologia Umana, 2nd Edition*. Rindi G, Manni E (Eds). Unione Tipografico-Editrice Torinese, Turin, Italy, 1149–1154 (1982).

42. Giuseppetti GM, Argalia G, Salera D, Ranaldi R, Danieli G, Cappelli M: Ultrasonographic contrast-enhanced study of sicca syndrome. *Eur. J. Radiol.* 54, 225–232 (2005).

43. Carotti M, Salaffi F, Manganelli P, Argalia G: Ultrasonography and colour doppler sonography of salivary glands in primary Sjögren's syndrome. *Clin. Rheum.* 20, 213–219 (2001).

44. Schroeder HG, Schwerk WB, Eichhorn T: High-resolution real-time sonography in salivary gland diseases. II. Salivary gland tumors. *HNO* 33, 511–516 (1985).

45. Izumi M, Eguchi K, Nakamura H, Nagataki S, Nakamura T: Premature fat deposition in the salivary glands associated with Sjögren Syndrome: MR and CT evidence. *Am. J. Neuroradiol.* 18, 951–958 (1997).

46. Stone DN, Mancuso AA, Rice D, Hanafee WN: Parotid CT Sialography. *Radiology* 138, 393–397 (1981).

47. Kawai Y, Sumi M, Kitamori H, Takagi Y, Nakamura T: Diffusion-weighted MR microimaging of the lacrimal glands in patients with Sjögren's syndrome. *Am. J. Roentgenol.* 184(4), 1320–1325 (2005).

48. Takagi Y, Sumi M, Sumi T, Ichikawa Y, Nakamura T: MR microscopy of parotid glands in patients with Sjögren's syndrome: quantitative MR diagnostic criteria. *Am. J. Neuroradiol.* 26(5), 1207–1214 (2005).

49. Tonami H, Ogawa Y, Matoba M *et al.*: MR sialography in patients with SS. *Am. J. Neuroradiol.* 19, 1199–1203 (1998).
•• Important article on magnetic resonance sialography.

50. Morimoto Y, Ono K, Tanaka T *et al.*: The functional evaluation of salivary glands using dynamic MR sialography following citric acid stimulation: a preliminary study. *Oral Surg. Oral Med. Oral Path. Oral Radiol. Endod.* 100(3), 357–364 (2005).

51. Morimoto Y, Habu M, Tomoyose T *et al.*: Dynamic MR sialography as a new diagnostic technique for patients with Sjogren's syndrome. *Oral Dis.* 12(4), 408–414 (2006).

52. Grevers G, Ihrler S, Vogl TJ, Weiss M: A comparison of clinical, pathological and radiologic findings with magnetic resonance imaging studies of lymphomas in patients with SS. *Eur. Arch. Otorhinolaryngol.* 251, 214–217 (1994).

53. Vitali C, Moutsopoulos HM, Bombardieri S: The European Community Study group on diagnostic criteria for Sjogren's syndrome. Sensitivity and specificity of tests for ocular and oral involvement in Sjogren syndrome. *Ann. Rheum. Dis.* 53, 637–647 (1994).

Affiliations

- *Susan I Lemon, DO*
  Scripps Clinic, Division of Rheumatology,
  10666 North Torrey Pines Road,
  Maildrop: MS113, La Jolla, CA 92037, USA
  Tel.: +1 858 554 8819;
  Fax: +1 858 554 6763;
  lemon.susan@scrippshealth.org

- *Steven G Imbesi, MD*
  Department of Radiology, Mail code # 8756,
  University of California, San Diego Medical
  Center, 200 W Arbor Drive, San Diego,
  CA 92103, USA
  Tel.: +1 619 543 6768;
  Fax: +1 619 543 3781;
  simbesi@ucsd.edu

- *Alexander R Shikhman, MD, PhD*
  Scripps Clinic, Division of Rheumatology,
  10666 North Torrey Pines Road,
  Maildrop: MS113, La Jolla, CA 92037, USA
  Tel.: +1 858 554 8562;
  Fax: +1 858 554 6763;
  ashikhman@scrippsclinic.com